



Interfacial reaction and microstructure between the Sn3Ag0.5Cu solder and Cu–Co dual-phase substrate

Chao Li¹ · Xiaowu Hu¹ · Xiongxin Jiang¹ · Yulong Li¹

Received: 25 April 2018 / Accepted: 7 June 2018 / Published online: 11 June 2018
© Springer-Verlag GmbH Germany, part of Springer Nature 2018

Abstract

In this study, interfacial reactions and microstructures of the Sn3Ag0.5Cu (SAC305)/Cu–*x*Co (*x*=0, 30 and 50 wt%) systems were investigated during reflowing at 290 °C and solid-state aging at 150 °C for various time. The effects of different contents of Co in substrate on interfacial reaction in SAC305/Cu–*x*Co system were discussed. It was found that the addition of Co into pure copper substrate to achieve alloying would effectively inhibit the growth of IMC layers. Comparison among the thickness of the intermetallic compound (IMC) in three kinds of SAC305/Cu–Co systems indicated that the IMC layer of SAC305/Cu joint was thicker than that of the other two types of solder joints. The composition of the SAC305/Cu IMC layers was Cu₆Sn₅ and Cu₃Sn. Three kinds of reaction phases (Cu,Co)₆Sn₅, (Cu,Co)Sn₂ and (Cu,Co)₃Sn were found at the interfaces of the SAC305/Cu-30Co and SAC305/Cu-50Co joints. Remarkably the (Cu,Co)Sn₂ phase was found adjacent to the Co-rich phase after soldering and eliminated after the aging treatment. While the (Cu,Co)₃Sn phase accumulated increasingly adjacent to the substrate with the increased aging time. The results suggested that the Co content increased from 30 to 50 wt% in substrate lead to significant restraint of the growth of interfacial IMC. In addition, the thickness of the interfacial IMC layer was linear with the square root of the aging time during the aging process. The reaction rate between Sn atoms in solder and Cu, Co atoms in substrate was quite different, which lead to the fact that the interface of SAC305/Cu–Co is uneven on the side of substrate after reflowing and aging.

1 Introduction

With the rapid development of electronic packaging technology, SnPb solder is being widely used in electronic packaging accessories and surface mount technology because of its excellent electrical conductivity, significant mechanical properties, good solder joint reliability and low price. However, solder alloys containing Pb have been proven toxic and its prohibited use is being implemented by stricter environmental policies. Therefore, in recent years, the industry has been focused on pursuing a new generation of lead-free solder that is good for sustainable development [1, 2]. As a result, the development of lead-free of electronic products is quite crucial. Nowadays, the most common lead-free solders are based on the Sn-rich or Sn–Ag-rich solder systems such as Sn–Cu solders, Sn–Zn solders, Sn–Ag solders, and

Sn–Ag–Cu solders [3–5]. Typically, from the point of view of reliability and solder cost, Sn3.0Ag0.5Cu (SAC305) solder is the most widely studied and used.

Some studies pointed that the thickness and the morphology of the IMC can impact the thermal fatigue life, isothermal shear fatigue life, tensile strength and fracture toughness. In the electronics industry, Cu is one of the most widely used metal substrate materials. The interfacial reactions between Sn-rich solder and Cu substrate have been studied by some researchers. However, numerous studies have shown that the interfacial reaction between SAC305 solders and Cu substrate is very intense after soldering and aging, which results in that the interfacial intermetallic compounds (IMCs) are generally too thick, leading the solder joint brittle and easy to fracture [6, 7]. Lee et al. [1] performed the solder joints of an Sn–Ag lead-free solder system with pure Cu wires. It has been demonstrated that the tensile strength of Sn–Ag system solder joints decreases as the thermal storage time increases, which may be attributed chiefly to the growth of interfacial Cu–Sn IMC layers. Hence, the formation of IMC has an important influence on the fractographic morphology and the tensile strength of the

✉ Xiaowu Hu
huxiaowu@ncu.edu.cn

¹ Key Lab for Robot and Welding Automation of Jiangxi Province, Mechanical and Electrical Engineering School, Nanchang University, Nanchang 330031, China

solder joints. In order to solve the above-mentioned issues, some trace elements such as Ag, Ga, Fe, Co and Ti have been added to the lead-free solder to improve the mechanical properties of the IMC [8–12]. Besides, there were some studies have indicated that the alloying of the metal substrate could also effectively inhibit the growth of the intermetallic compounds. Some studies have shown that the addition of Ni, Zn and other elements in the copper substrate could inhibit the growth of interfacial compounds [13–15].

In recent years, Co and its based alloys were regarded as alternative materials for diffusion barrier and wetting layers because of its good wettability and low solubility. Peng Sun et al. [16] reported that the thicknesses of the interfacial IMCs for Sn–Co–Cu solders was thinner than that of Sn–Ag–Cu solders. Previous studies indicated that Ni–Co alloys are regarded as diffusion barriers, and Co is another diffusion barrier layer material of UBM [17, 18]. Therefore, Cu–Co alloys may also be potential materials as an alternative diffusion barrier layer in the field of electronic packaging. In addition, some researchers reported that the growth of the intermetallic compound of the Sn/Cu–Co couples is effectively inhibited and the wettability is better than that of Sn/Co couples [19]. However, there was still a lack of research about that the effect of adding Co in Cu substrate on the interfacial reaction. Therefore, in this study, we focused on the interfacial reactions and IMC growth between the Sn3Ag0.5Cu solders and the Cu–Co dual-phase substrate during the soldering and solid-state isothermal aging.

2 Experimental procedures

In this study, three types of reaction couples of SAC305/Cu–*x*Co (*x*=0, 30 and 50 wt%) were prepared. Sn3Ag0.5Cu (in mass percent) solder balls with diameter of 0.6 mm were used in this experiment. For the Cu–Co alloys substrate, they were prepared by melting pure Cu and Co (with 99.99% purity) together in a vacuum induction furnace, according to their proper weight percentage. These prepared substrates were cut into a piece shape with a diameter of 15 mm and 2 mm in thickness. The Cu–Co substrates surface were polished by sandpaper and diamond paste, and then rinsed in deionized water. In order to observe the microstructure of prepared Cu–Co alloys, an etchant solution of 3% HCl + 5% HNO₃ + 92% CH₃OH was adopted. The microstructures of Cu–Co alloys were observed by using the optical microscope. At the beginning of reflow process, a certain number of SAC305 solder balls were reflowed with Cu–*x*Co (*x*=0, 30 and 50 wt%) substrates at 290 °C for 10 min. All the reflowed samples were finished under the same reflowing profile and then cooled in air.

In the field of electronic packaging, the reliability of solder joints is an important research content. Particularly, the

temperature of electronic component during service has a great influence on the quality of solder joint. Some studies reported that the Sn–Ag–Cu/Cu solder joints after aging treatment at 150 °C for 100 h can absorb higher impact energy at high-strain rate mechanical testing. In order to accelerate the microstructure coarsening, the aging temperature should be set near the melting point of solder [20]. In this experiment, after reflowing, the SAC305/Cu–*x*Co (*x*=0,30,50) couples were aged at 150 °C for 24, 120, 240 and 360 h, respectively. After the isothermal aging treatment, the samples were cut into proper size. Next, these samples were mounted in epoxy and then polished using 2.5 and 1.5 μm diamond paste. Finally, these samples were etched with a solution of 3% HCl + 5% HNO₃ + 92% CH₃OH and then metallographically observed the cross-sectional microstructure. The microstructures and reaction phase compositions were observed and determined by using Scan Electron Microscopy (SEM, FEI QUANTA 200F) and Energy Dispersive Spectrometer (EDS with acceleration voltage of 20 KV).

Due to the uneven distribution of the thickness of the intermetallic compound, the area value of the IMC layer is taken by the image software, and the total thickness of the IMC is calculated by the formula (1):

$$H_{\text{IMC}} = (M_{\text{IMC}}/M_{\text{SEM}}) \times H_{\text{SEM}}, \quad (1)$$

where H_{IMC} is the actual thickness of the IMC, and H_{SEM} is the actual height of the SEM micrograph. The M_{IMC} represents the pixel in the IMC layer photo and M_{SEM} is the total pixel of the SEM image. In order to reduce the error of the measured statistics between the various couples, the thickness of IMC for each group of samples tested were obtained by analyzing at least fifteen measurements and taking the average. Meanwhile, in order to improve the accuracy of the experiment, five specimens under the same conditions for each sample tested were also prepared.

3 Results and discussions

For a comparison, the experiment of interface reaction between SAC305 and pure copper substrate was conducted. Figure 1 shows the cross-sectional micrographs of the interfacial microstructure between SAC305 and pure copper substrate with different aging time at 150 °C. Figure 1a shows the result of the SAC305/Cu couples without solid-state aging treatment after soldering. The average thickness of the total reaction layer was about 6.94 μm. It was clearly seen that there were two continuous reaction layers of Cu–Sn IMC found simultaneously at the interface. Close to the side of the solder was the Cu₆Sn₅ phase with different thickness, and the phase composition adjacent to the Cu substrate was determined to be Cu₃Sn, similar to the research of Hu et al.

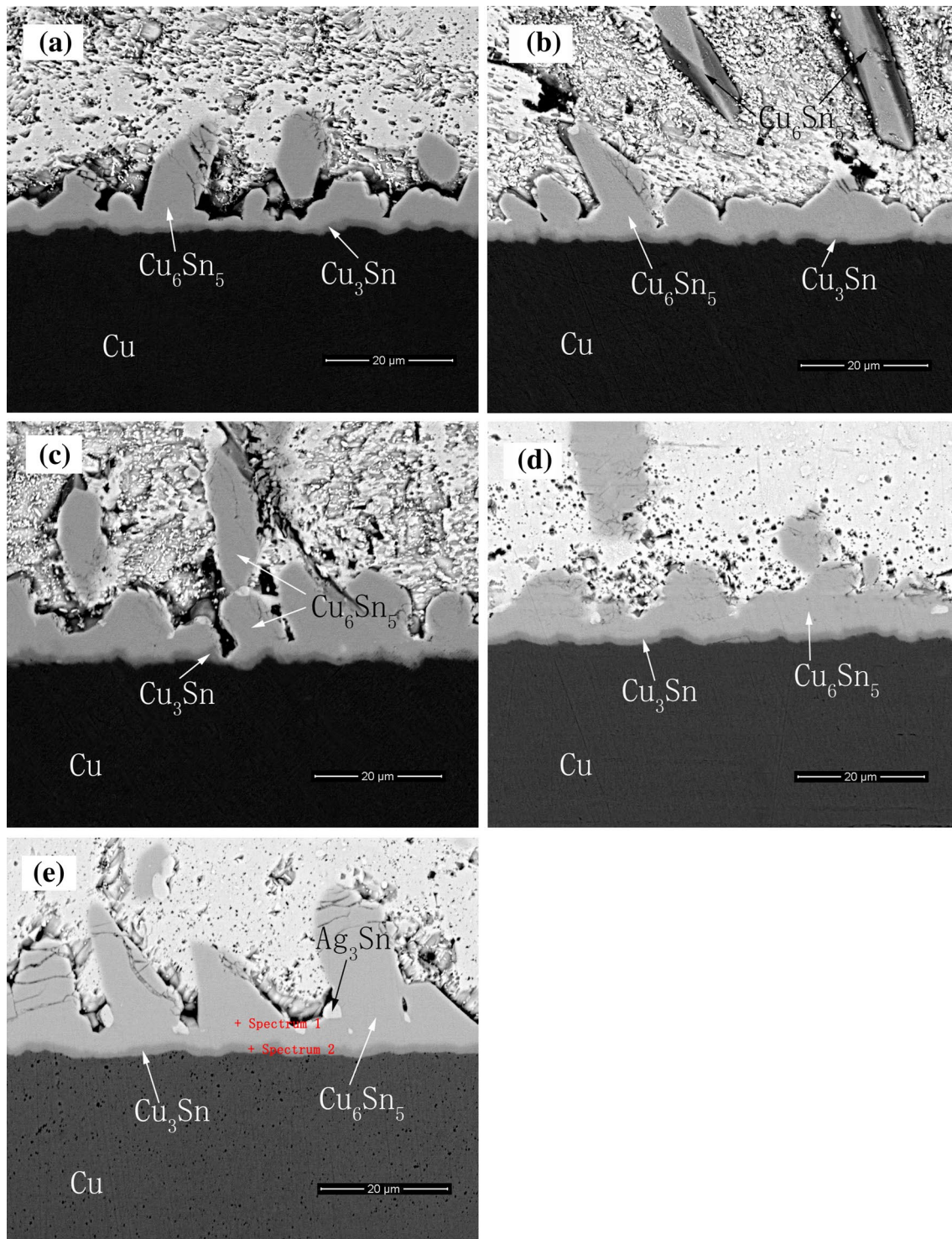


Fig. 1 Cross-sectional micrographs of SAC305/Cu joint under different aging times. **a** 0, **b** 24, **c** 120, **d** 240, **e** 360 h

[21]. These results verified that the scallop-like Cu_6Sn_5 phase was the dominate phase and the thickness of Cu_3Sn phase was quite small after the liquid–solid interfacial reaction at the 290 °C for 10 min. Figure 1b–d shows the total thickness of Cu_6Sn_5 and Cu_3Sn phases after solid-state aging

at 150 °C for 24, 120, and 240 h, respectively. It was indicated that the IMC thickness increased with increasing aging time and a small amount of the Cu_6Sn_5 phase were observed in the solder matrix due to the diffusion of Cu atoms from the substrate. Figure 1e shows the interfacial microstructure

of SAC305/Cu solder joint aged at 150 °C for 360 h. The average thickness of the total IMC increased dramatically to 13.21 μm . Obviously, after the aging treatment, the thickness of the interfacial compound increased significantly. The results of the EDS are shown in Fig. 2. Figure 2a shows that the light phase closed to the solder was Cu_6Sn_5 composed of 55.18 at% Cu and 44.82 at% Sn. Figure 2b shows that the gray phase adjacent to the substrate was determined to be Cu_3Sn with composition of 74.28 at% Cu and 25.72 at% Sn. Typically, as shown in Fig. 1e, Ag_3Sn was observed adjacent to the Cu_6Sn_5 phase because of the aggregation of Ag element after aging. The reason for this phenomenon was

that some Sn atoms were consumed near the interface of Cu_6Sn_5 /solder to form Cu_6Sn_5 , which reduced the content of Sn atoms and increased the content of Ag atoms near the Cu_6Sn_5 phases, causing Ag_3Sn to form and aggregate with aging treatment. Some studies have shown that the Ag_3Sn IMC in solder matrix might affect the mechanical integrity of the solder assembled in flip-chip joints [22].

By using the optical microscope, the microstructures of fabricated Cu–Co alloy with 30 wt% Co and 50 wt% Co are shown in Fig. 3 a, b, respectively, in which the Cu-rich phase is bright and the Co-rich phase is dark. It can be observed that this composite substrate has a distinct dual-phase

Fig. 2 EDS analysis of IMCs between solder and substrate, **a** EDS pattern of spectrum 1, and **b** EDS pattern of spectrum 2 in Fig. 1e

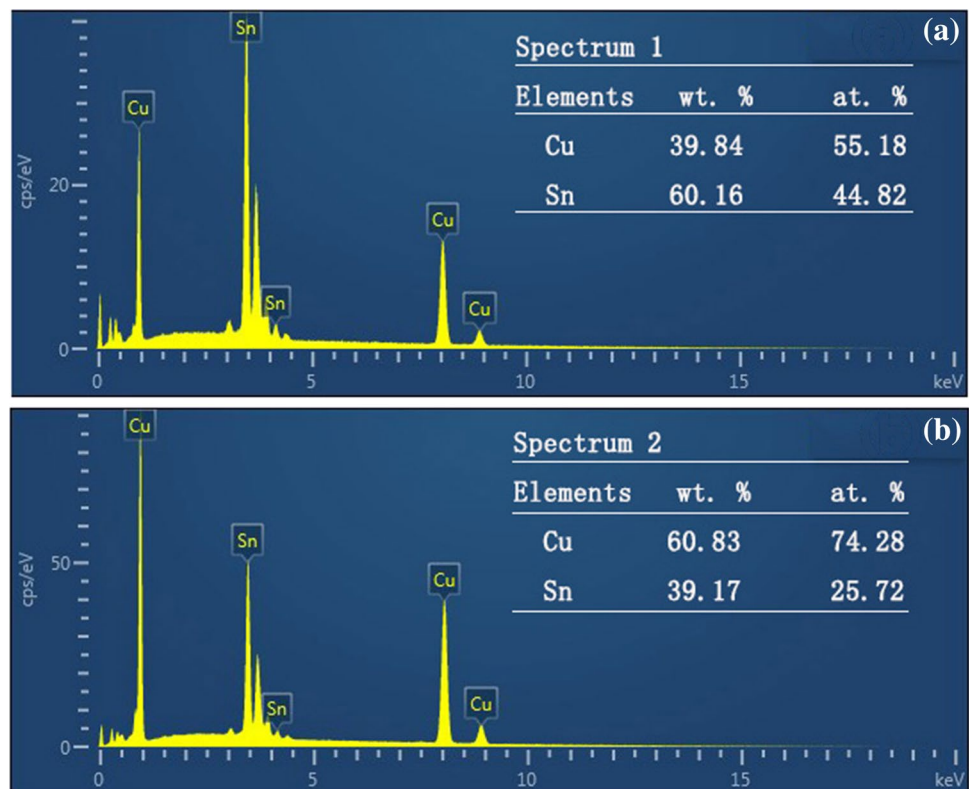
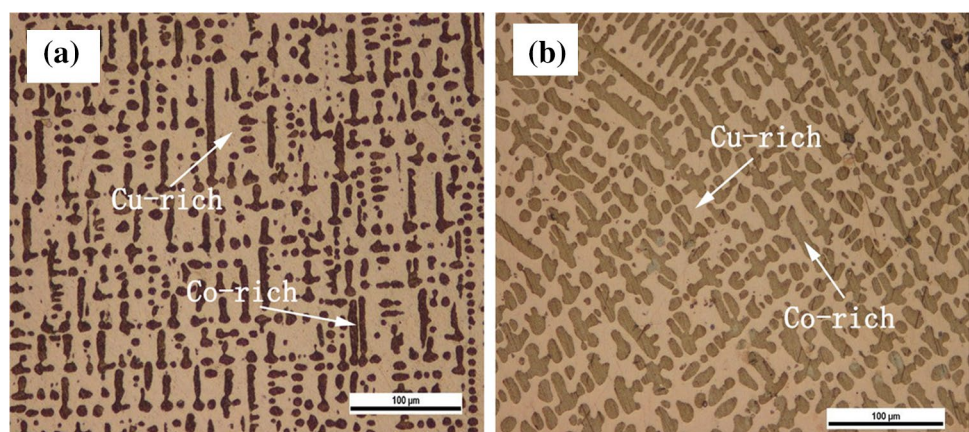


Fig. 3 Microstructure of the Cu–Co alloy. **a** Cu-30 wt% Co, **b** Cu-50 wt% Co



microstructure consisting of Co-rich phase embedded the Cu-rich phase. By using image software analysis, the surface fraction of the Co-rich phase in Cu-30Co and Cu-50Co alloy was approximately 0.27 and 0.48, respectively.

In order to clarify the effect of Co content in substrate on the interfacial reaction between SAC305 solder and Cu–Co substrate, there were two sets of joints of SAC305/Cu-30Co and SAC305/Cu-50Co were fabricated. Figure 4a–e shows

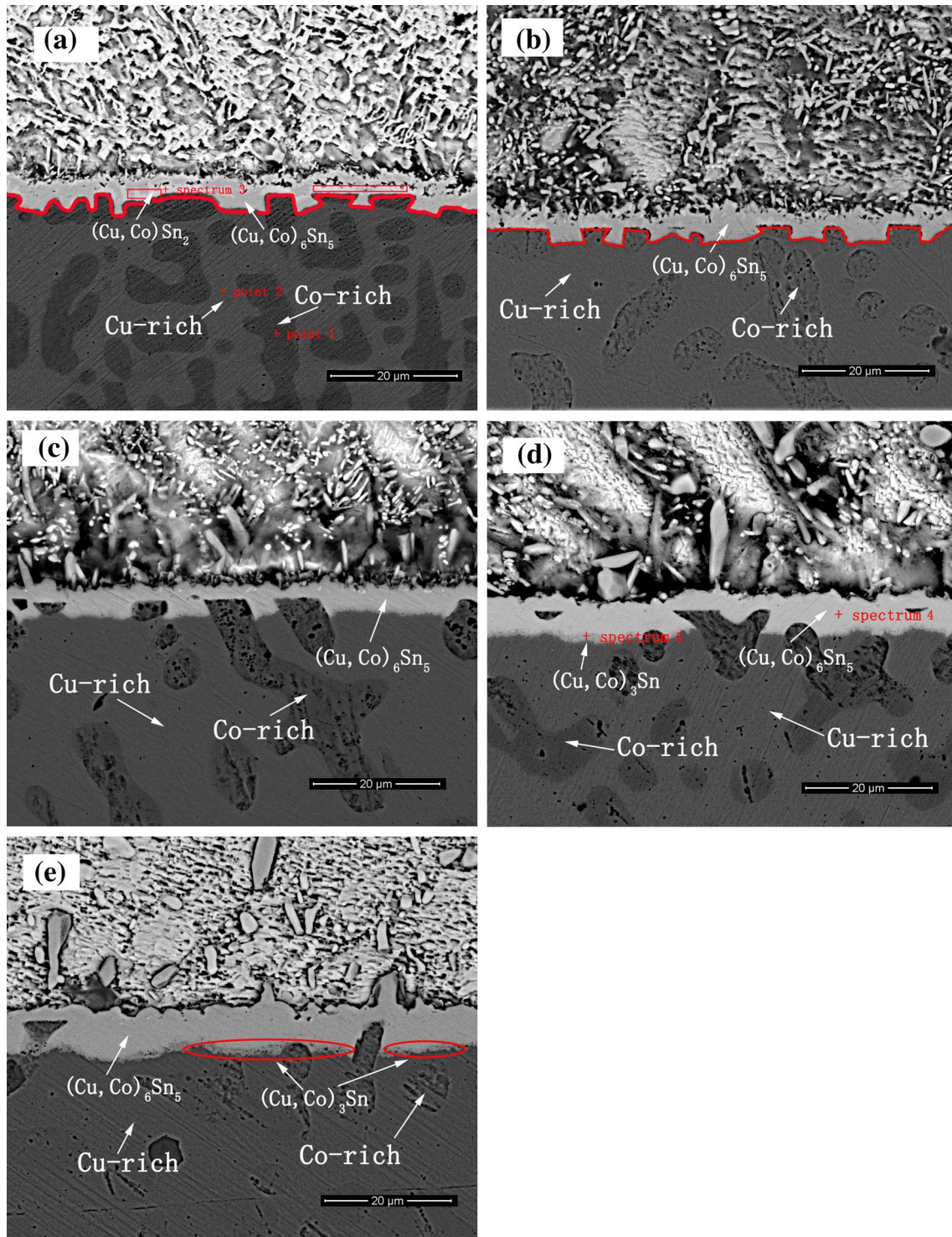


Fig. 4 Cross-sectional micrographs of SAC305/Cu-30Co joint under different aging times. **a** 0, **b** 24, **c** 120, **d** 240, **e** 360 h

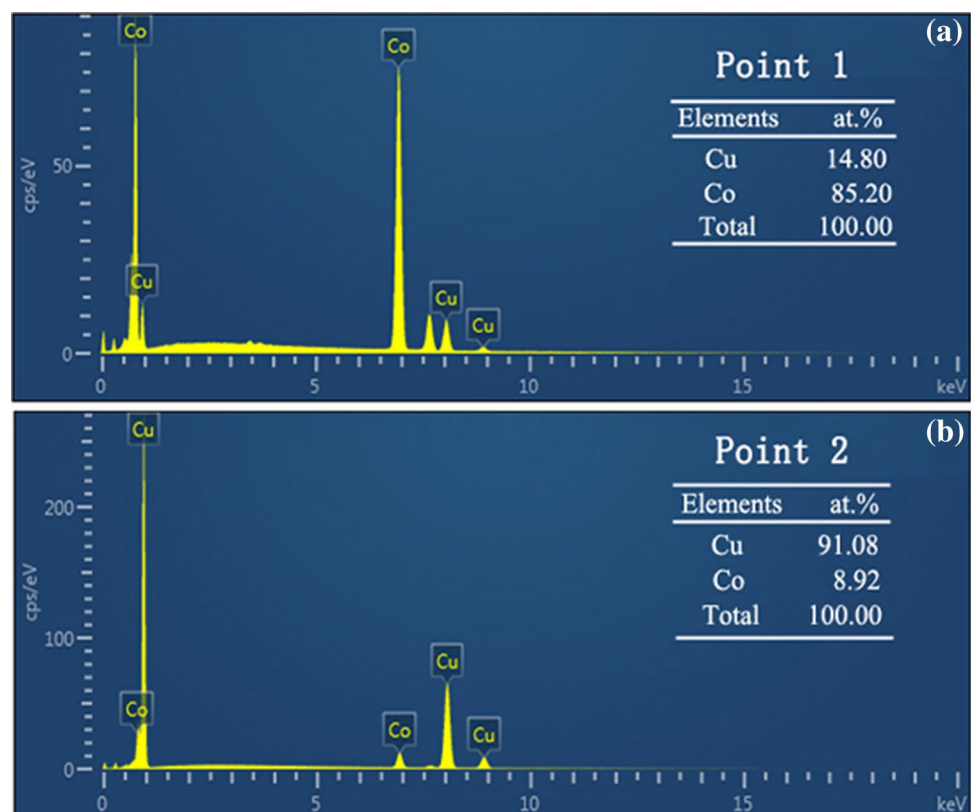
the interfacial microstructures of SAC305/Cu-30Co joint with various aging time.

The observed result of the interfacial microstructure between liquid solder and Cu-30Co substrate is presented in Fig. 4a. As shown in Fig. 4a, two phases (Cu-rich and Co-rich) can be seen in Cu-Co alloy substrate. Figure 5a, b presents the detailed compositions of those two phase, as indicated by point 1 and point 2 in Fig. 4a. Some studies had been reported that the coexistence of Cu-rich solid solution and Co-rich solid solution phases in Cu-50Co alloys was observed. The crystal structure of these two phases is fcc [23–26].

After soldering, it was obviously seen that there were two reaction layers were formed at the interface. The continuous dark phase composition was determined to be $(\text{Cu},\text{Co})_6\text{Sn}_5$ which meant Cu_6Sn_5 phase with high Co content. The light phase composition adjacent to the Co-rich phase was identified as 25.25 at% Co, 6.19 at% Cu and 68.56 at% Sn (indicated as spectrum 3 and square shown in Fig. 4a) and denoted as $(\text{Cu},\text{Co})\text{Sn}_2$, which was very thin and discontinuous. The reason for the formation of these two reaction products was that there were enough Sn atoms to react with Cu atoms and Co atoms during soldering resulting in forming two compounds $(\text{Cu},\text{Co})_6\text{Sn}_5$ and $(\text{Cu},\text{Co})\text{Sn}_2$. The average thickness of the total IMC was approximately 2.24 μm , which was much smaller than that of the SAC305/Cu joint (6.94 μm). This observation illustrated that the addition of

Co into pure copper substrate could inhibit the growth of the whole IMC layer. As seen from red lines in Fig. 4a, b, a dense solder joint formed between the liquid Sn-based solder and bi-phase Cu-Co substrate with irregular shape adjacent to the substrate. The reason for this phenomenon was that the Co element was added to the copper substrate. Moreover, since the reaction rate of the liquid Sn with the Cu-rich phase was much higher than that with the Co-rich phase, the Cu-rich phase on the surface of the substrate was rapidly consumed, resulting in uneven surface and a large number of microchannels adjacent to the substrate marked, as red lines shown in Fig. 4a, b. It was found that the solubility of Cu and Co in liquid Sn was about 11 and 0.5 at.% at the temperature of 400 °C, so the reaction rate between two phases (Cu-rich and Co-rich phases) and the liquid Sn was quite different [27]. It is well known that the substrate roughness is favorable for solder wetting in the field of electronic packaging. Studies developed by Satyanarayan et al. [28, 29] pointed out that the wetting properties of two kinds of solders (including SAC387 and Sn-0.7Cu) on the surface of Cu substrate in detail. They found that the liquid solder wetting performance on the rough Cu substrate is significantly better than that on smooth Cu substrate. There were also some studies on the wetting properties of liquid solders with dual-phase substrates. The research proposed by Lai et al. [30] indicated that the dissolution could also affect wettability in IMC-forming systems when dual-phase

Fig. 5 EDS analysis of Cu-30Co alloy substrate. **a** Point 1 in Fig. 4a, **b** Point 2 in Fig. 4a



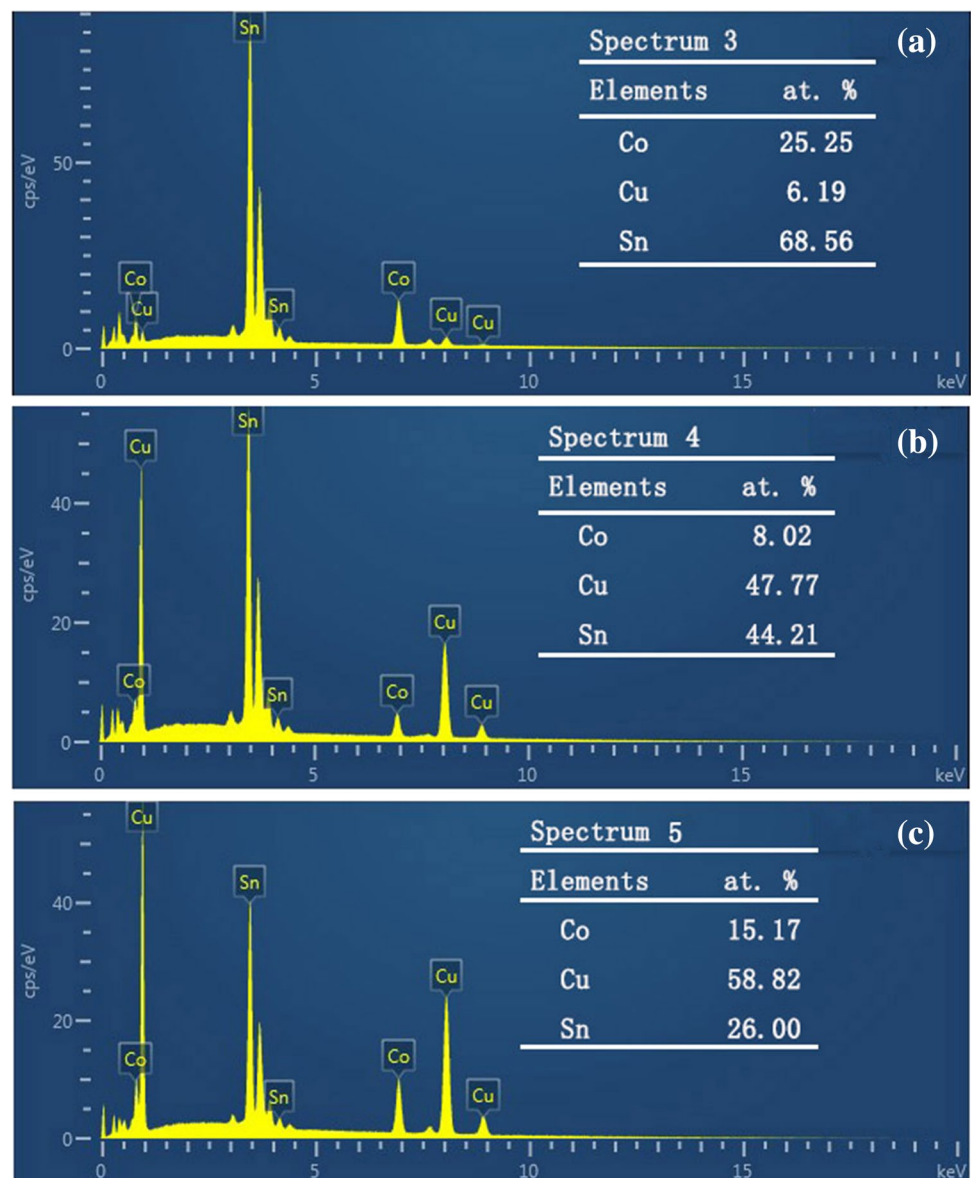
substrates were involved. They found that the enhanced wettability was attributed to the dissolution contrast between the solid components leading to increasing roughness of the substrate, thus providing an additional driving force for wetting. Therefore, an in-depth study of this uneven interface between solder and dual-phase substrate is quite necessary for industrial applications in the future.

Figure 4b–e displays that the average thickness of the total IMC was increasing with the aging time increases. There were two layers appeared in Fig. 4d. The dark phase adjacent to the substrate was much thinner than the light layer. Figure 6b shows that the light phase composition was identified as 8.02 at% Co, 47.77 at% Cu and 44.21 at.% Sn, conforming it to be $(\text{Cu,Co})_6\text{Sn}_5$. Figure 6c shows that the dark layer adjacent to the substrate was $(\text{Cu,Co})_3\text{Sn}$ composed of 15.17 at% Co, 58.52 at% Cu and 26.00 at.% Sn. It

could be known that the Co content in $(\text{Cu,Co})_3\text{Sn}$ at spectrum 5 was higher than that for $(\text{Cu,Co})_6\text{Sn}_5$ at spectrum 4. This means that the more Co trend to accumulate at the interface near the side of substrate with the aging treatment. According to literature, Chen et al. [31] pointed that Co atoms in the CoSn_3 layer were partly substituted by Cu and Pd atoms from the solder and substrates to form $(\text{Co,Cu,Pd})\text{Sn}_3$. Similar to our study, in which the $(\text{Cu,Co})_3\text{Sn}$ IMC rather than Cu_3Sn IMC formed at the interface in our experiments due to Cu atoms in Cu_3Sn IMC were partly replaced by Co atoms.

In addition, some Cu_6Sn_5 phases were found inside the solder, because Cu atoms diffused into the solder from the substrate during the aging treatment. Figure 4e shows the results of the IMC morphology aged at 150 °C for 360 h. Similar to the interfacial reaction between SAC305 solders

Fig. 6 EDS analysis of IMCs between solder and substrate, **a** EDS pattern of spectrum 3 in Fig. 4a, **b** EDS pattern of spectrum 4, and **c** EDS pattern of spectrum 5 in Fig. 4d



and pure copper substrate, the thickness of the $(\text{Cu},\text{Co})_6\text{Sn}_5$ and $(\text{Cu},\text{Co})_3\text{Sn}$ phase increased with increasing aging time.

In the initial stage of aging treatment, there were enough Sn atoms that adjacent to Co-rich phase to react with Co atoms to form CoSn_2 . However, due to a small amount Cu atoms occupy the part of Co atoms in Co-rich phase, eventually resulting in the formation of the $(\text{Co},\text{Cu})\text{Sn}_2$ phase. According to Chen et al.'s study, Sn/Ni-20at%Co couple reacted at 250 °C for 10 min could form the CoSn_2 phase with composition of Sn-22.3at%Ni-10.4at%Co [17]. Whereas, with the aging treatment, the content of $(\text{Cu},\text{Co})\text{Sn}_2$ phase became less and less so that it was not easy to found. It might be the dark $(\text{Cu},\text{Co})_6\text{Sn}_5$ phase formation would vastly consume the Sn atoms and act as a barrier layer to against Sn atoms diffusion. Previous studies reported that $(\text{Cu},\text{Co})_6\text{Sn}_5$ phase is more stable than Cu_6Sn_5 in Sn-0.7 wt%Cu/Co interface solder [34]. That is, the Co atoms preferably occupy the Cu sublattice sites of Cu_6Sn_5 , which might result in a more stable phase $(\text{Cu},\text{Co})_6\text{Sn}_5$ formation. As a result, there were not enough Sn atoms for reacting with Co atoms to form $(\text{Cu},\text{Co})\text{Sn}_2$ phase and the dominant component of IMC was $(\text{Cu},\text{Co})_6\text{Sn}_5$ phase. In addition, the difference in the reaction rate of Cu atoms and the Co atoms with the Sn atoms, respectively became insignificant with the aging treatment.

As exhibited in Fig. 7, a similar experiment was carried out by replacing the substrate part with Cu-50Co. It can be seen that the Cu-50Co substrate had more Co-rich phase than the Cu-30Co substrate.

Similar to Fig. 4a, there were two reaction layers that ($(\text{Cu},\text{Co})_6\text{Sn}_5$ and $(\text{Cu},\text{Co})\text{Sn}_2$ phases) were formed at the interface, as shown in Fig. 7a, while the $(\text{Cu},\text{Co})_6\text{Sn}_5$ was still the dominant reaction layer between the solder and Cu-50Co substrate and little $(\text{Cu},\text{Co})\text{Sn}_2$ phase was adjacent to the Co-rich phase. Compared these two kinds joints (SAC/Cu-30Co and SAC/Cu-50Co), the measured thickness of IMC (1.97 μm) in Fig. 7a was thinner than that in Fig. 4a (2.24 μm). This demonstrated that the average thickness of the total reaction layer became thinner as the content of Co increased from 30 to 50% in substrate. As a result, Co would affect the formation of $(\text{Cu},\text{Co})_6\text{Sn}_5$ phase to restrain the growth of the total IMC. In following aging treatment process, the IMCs became thicker with aging time increased. The results of the chemical composition analysis of IMC layers by using EDS are shown in Fig. 8. The spectrum 6 was determined to be $(\text{Cu},\text{Co})_6\text{Sn}_5$ phase with 10.9 at% Co, 43.83 at% Cu and 45.27 at.% Sn and spectrum 7 was regarded as $(\text{Cu},\text{Co})_3\text{Sn}$ phase composed of 16.38 at% Co, 58.73 at% Cu and 24.89 at.% Sn. It was clearly shown that the content of Co increased from 10.9 at% to 16.38 at% at the interface adjacent to the substrate to form the $(\text{Cu},\text{Co})_3\text{Sn}$ phase. It was observed that the interfacial microstructure was still uneven despite through aging treatment for 240 and 360 h,

as shown in Fig. 6d and e, due to the consuming rate of Cu was faster than that of Co in the Cu–Co substrate close to the interface. In other words, the more content of Co in substrate caused the less Cu atoms to be consumed. Moreover, comparing the thickness of reaction layers formed by the two kinds of joints (SAC305/Cu-30Co and SAC305/Cu-50Co), results indicated that the average thickness of overall IMC of SAC305/Cu-50Co joint was thinner due to the Co content increased in the substrate. For displaying the effect of Co content in the substrate on the thickness of IMCs, the thickness of IMCs for various joints at different aging time is demonstrated in Table 1 and Fig. 9, respectively.

Table 1 lists the average thickness of the SAC305/Cu–xCo solder joints with different aging time. At the same time, Fig. 9 shows a graphical representation of the changes in the thickness of IMCs with increased aging time for all solder joints. It could be seen from the growth curve in Fig. 9 that both of the IMC thickness of the SAC305/Cu-30Co and SAC305/Cu-50Co couples increased with the increasing aging time. However, as shown in Fig. 9, referring to the average thickness of interfacial reaction layers in SAC305/Cu system, the average thickness of interfacial reaction layer in both SAC305/Cu-30Co and SAC305/Cu-50Co systems were significantly suppressed, resulting in a quite thin IMC layer.

Particularly, the interfacial IMC layer thickness of SAC305/Cu-50Co system was much thinner than that of SAC305/Cu-30Co. It was obvious that the higher the Co content in the substrate, the more conspicuous inhibition of the IMC thickness. In addition, comparing three kinds of solder joints, the growth rate of SAC305/Cu interfacial IMC was the faster than that of other two joint systems. Especially, discussing the growth behaviours of interfacial IMC layers of SAC305/Cu-30Co and SAC305/Cu-50Co solder joints in Fig. 9, their interfacial reaction layers had almost the same growth rates in the initial stage. With the processing of solid-state aging treatment, SAC305/Cu-50Co growth rate was lower than that for SAC305/Cu-30Co.

Exploring the cause of this phenomenon, the diffusion of the Sn atoms dominated the growth of the interfacial IMCs at the soldering stage when Sn atoms preferentially combined with Cu atoms to form the Cu–Sn compounds. As for the interfacial reaction between the SAC305 solder and Cu–Co alloy substrate, the rate of Cu consume was faster than that of Co. In the solid-state aging process, Co could diffuse from the substrate to the interfacial compound to form the $(\text{Cu},\text{Co})_6\text{Sn}_5$ and $(\text{Cu},\text{Co})_3\text{Sn}$. Although the content of Co was increased, while the content of Cu was decreased in substrate, the growth of the overall interfacial compound thickness was restrained due to the less formation of Cu–Sn compounds. In summary, alloying substrate could inhibit the growth of interfacial IMC. The more Co content added in the Cu substrate, the more obvious inhibition effect on

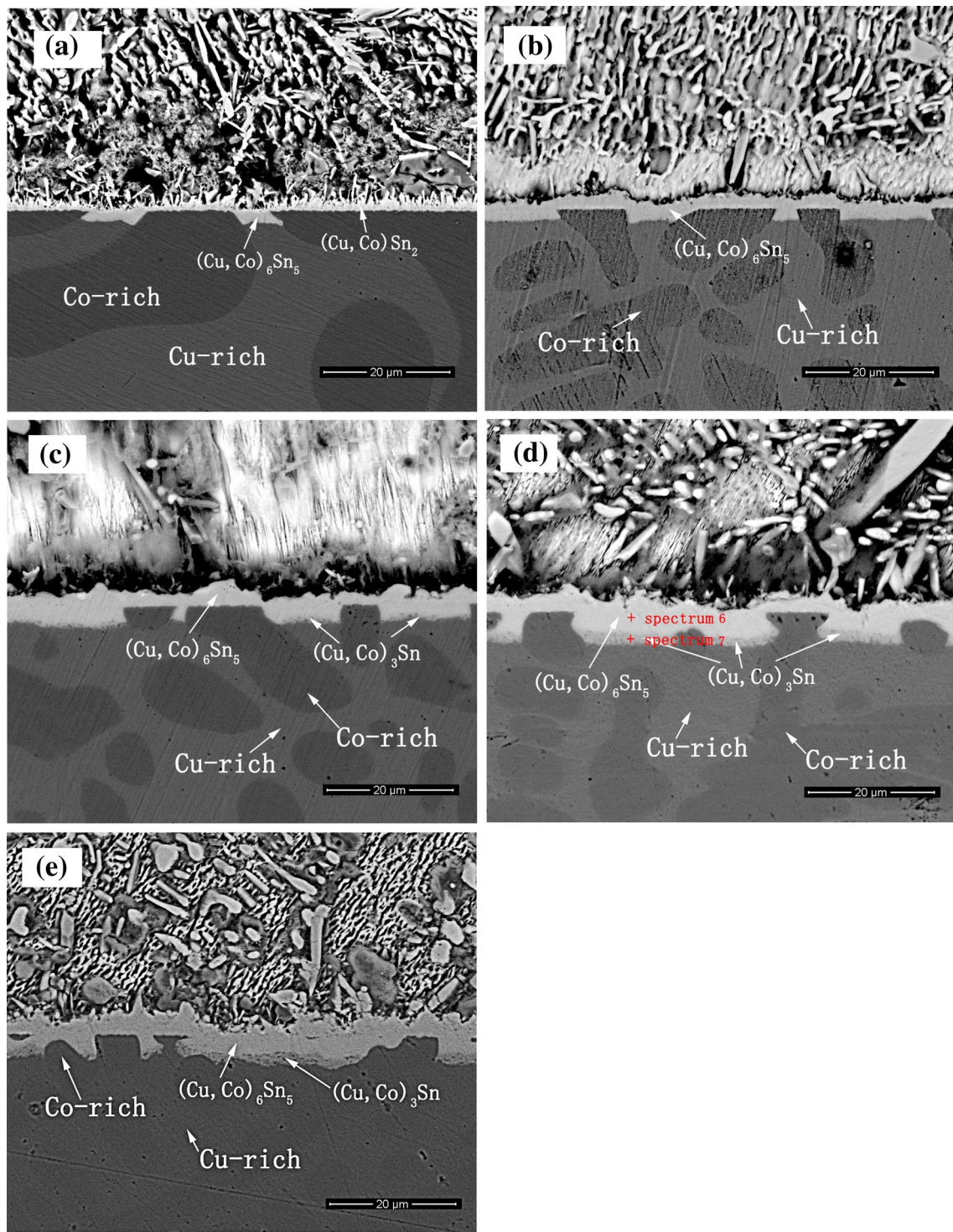


Fig. 7 Cross-sectional micrographs of SAC305/Cu-50Co joint under different aging times. **a** 0, **b** 24, **c** 120, **d** 240, **e** 360 h

the growth of the interfacial IMC layer. Figures 10 and 11 show the element maps of the cross-sectional micrographs of the SAC305/Cu-30Co joint and the SAC305/Cu-50Co joint. In these pictures, it clearly seen that the distribution of elements at SAC305/Cu–Co interface after aging at 150 °C

for 240 h. Cu and Co elements were aggregated to form the Cu-rich and Co-rich phases in the alloy substrate, respectively. Sn elements were found in solder and IMC reaction layers. Moreover, from the picture it can be seen that lots of Ag atoms were aggregated in the form of Ag₃Sn phase and

Fig. 8 EDS analysis of IMCs between solder and substrate, **a** EDS pattern of spectrum 6, and **b** EDS pattern of spectrum 7 in Fig. 7d

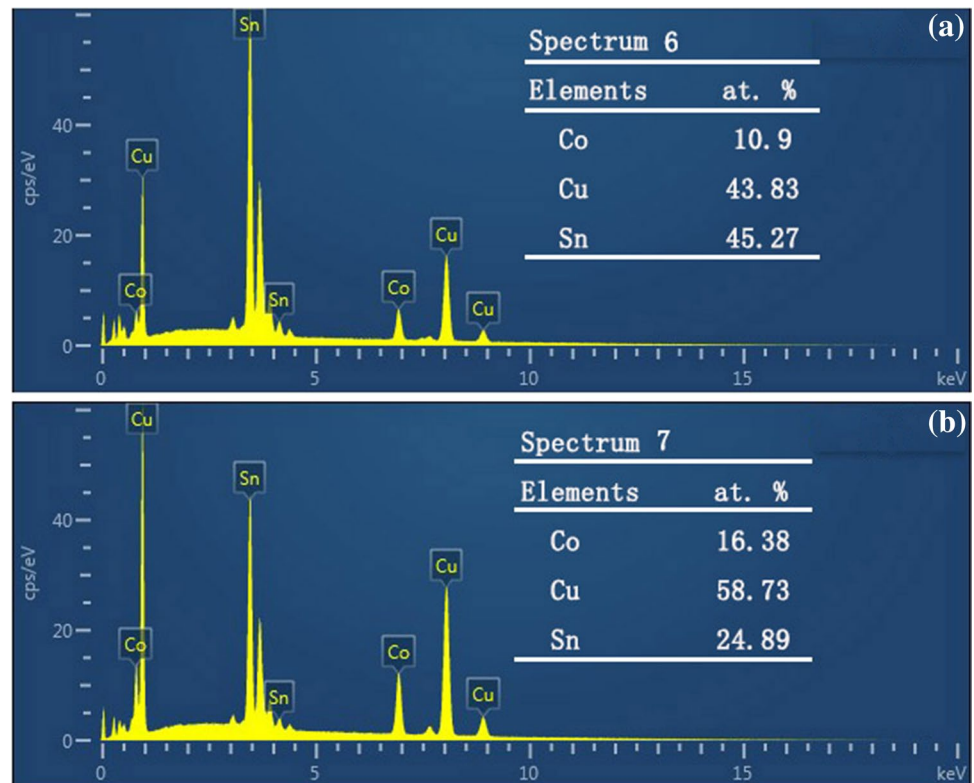


Table 1 Results of statistical analysis for the IMC thickness in the aged SAC305/Cu–Co couples

Aging time/h	0	24	120	240	360
SAC/Cu IMC thickness/ μm	6.94	7.87	10.85	12.44	13.21
SAC/Cu-30Co IMC thickness/ μm	2.24	3.23	6.32	7.28	7.97
SAC/Cu-50Co IMC thickness/ μm	1.97	2.59	3.58	4.61	5.32

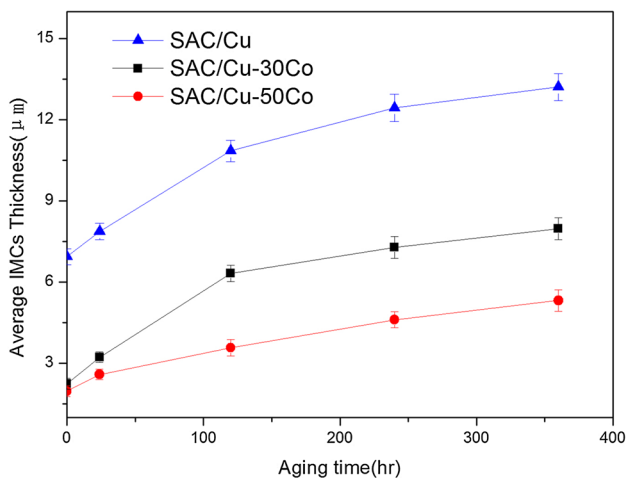


Fig. 9 Thickness of the SAC305/Cu– x Co reaction layers under different aging times

widely distributed in solder matrix after aging. The quality of the solder is an important factor on affecting the reliability of the joint. According literature [32], the shear strength of SnAgCu solder joints was primarily dependent on the size and distribution of Ag_3Sn distribution. In general, the finer the dispersions are, the higher strength the bulk solder has. As a result, the Ag_3Sn phase in solder would indirectly affect the reliability of the joint. Besides, according to previous study, Cu–Sn IMC in the solder also played an important role in both the microstructure evolution and failure of solder joints [33]. Former researcher reported that the bulky Cu_6Sn_5 phase was also detected in solder. That indicated that after soldering, the Cu atoms diffused into the molten solder to form Cu_6Sn_5 phases that tend to conglomerate during high temperature aging [34]. Similar to our experimental results that Cu atoms can be found in the solder, while Co atoms not be found in the solder as shown in EDS map.

Figures 10 and 11 obviously show the morphology of the IMC at SAC305/Cu–Co interface adjacent to the substrate. In the initial stage of soldering, Cu atoms reacted with Sn atoms at the interface, which resulted in that the Cu-rich phases were consumed quickly. Meanwhile, in that condition, the consuming rate of Co atoms was lower than that of Cu atoms, which was the reason why the interface close to the substrate was uneven and showed jagged-shape, similar to the red lines in Fig. 4a, b.

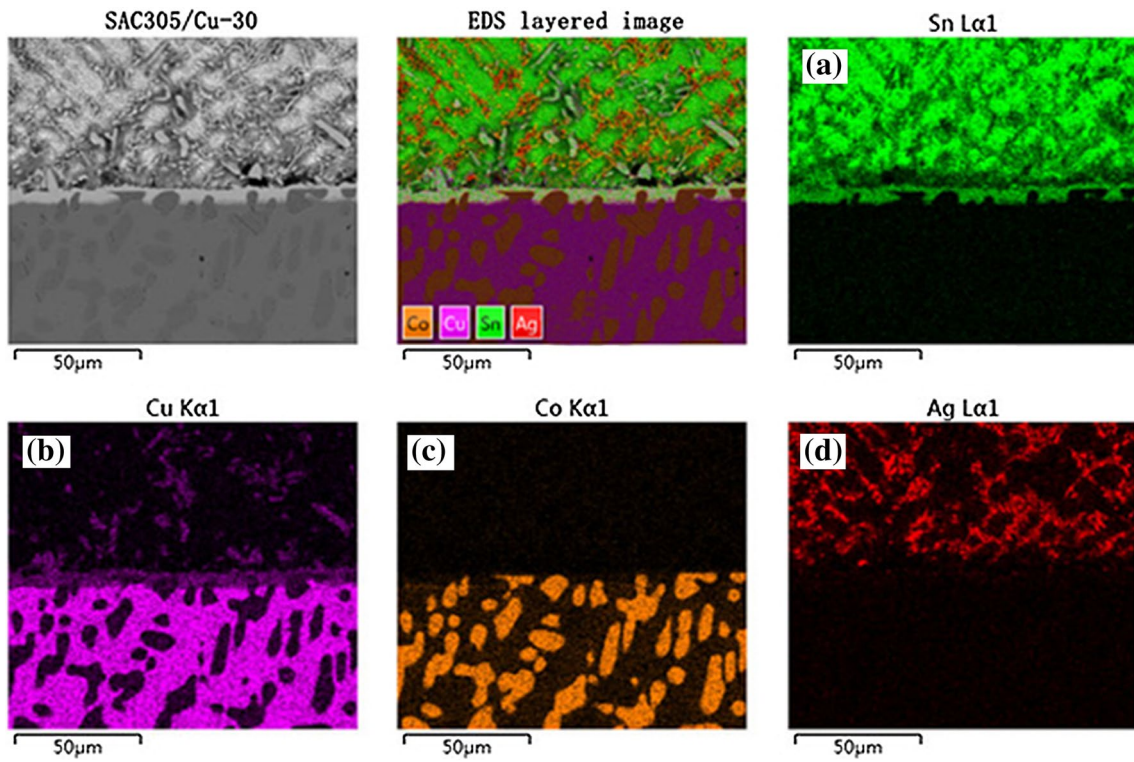


Fig. 10 Elemental maps of the SAC305/Cu-30Co interface after aging at 150 °C for 240 h. **a–c** and **d** show the elemental distribution map of Sn, Cu, Co and Ag, respectively

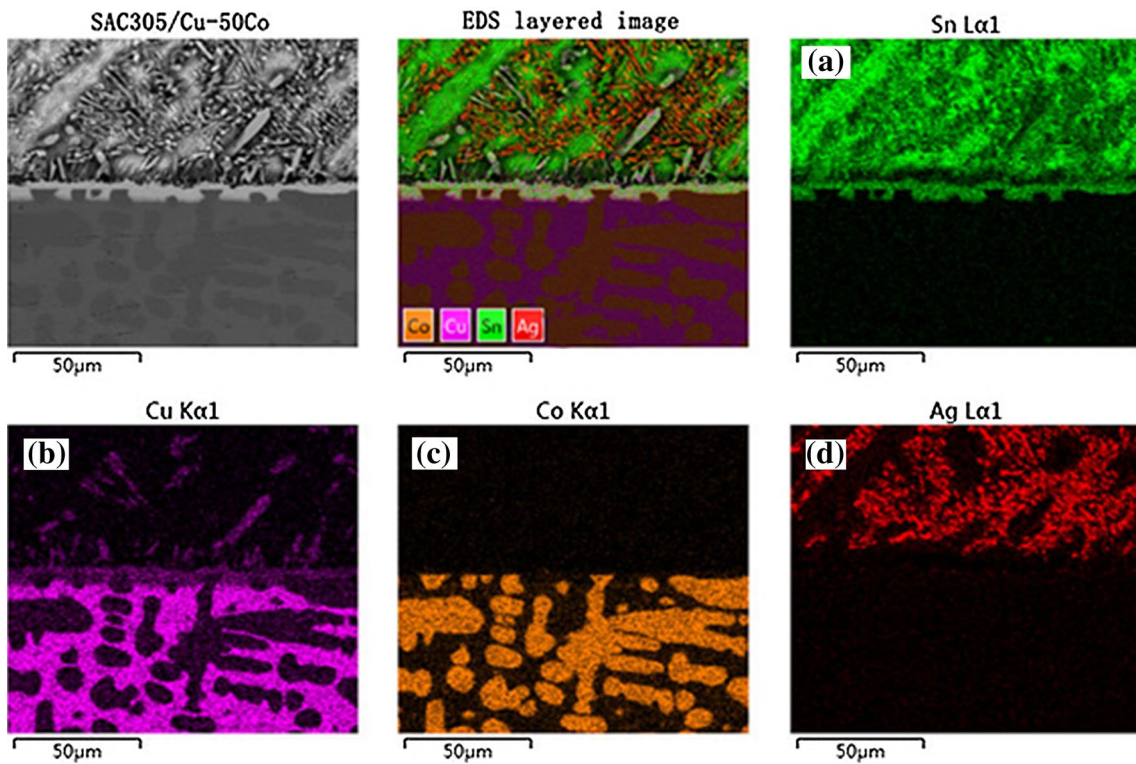


Fig. 11 Elemental maps of the SAC305/Cu-50Co interface after aging at 150 °C for 240 h. **a–c** and **d** show the elemental distribution map of Sn, Cu, Co and Ag, respectively

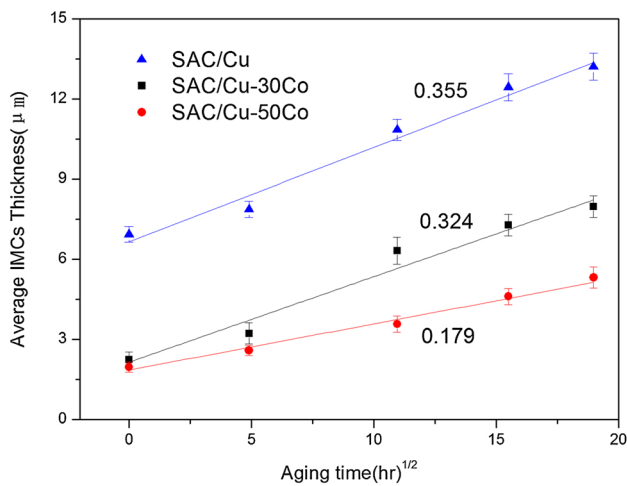


Fig. 12 Thickness of the IMC of SAC305/Cu- x Co joints with the square root of aging time

The thickness of the reaction layers formed during the aging treatment can be described by the following formula [35]:

$$X = X_0 + kt^n, \quad (2)$$

where X_0 is the initial thickness of reaction layer after soldering, X is the reaction layer thickness at aging time t . k is the growth rate constant and n is the time exponent. Previous study has shown that the time index of n represents the layer growth type and possible reaction mechanism of the interfacial compound during aging treatment [36]. In addition, when the IMC growth follows the linear kinetics, the growth rate is controlled by the reaction rate of the growth site. When the IMC growth is controlled by volume diffusion, the parabolic growth kinetics are followed [35]. As for diffusion control mechanism, the growth of the IMC layer thickness after aging treatment would follow the parabolic growth that it is diffusion-limited and the value of n is 0.5 [37].

The relationship between square root of the aging time and the thickness of the interfacial IMC by fitting to obtain the curve is shown in Fig. 12. It could be seen that the thickness of reaction layers in the SAC305/Cu- x Co joints was linearly related to the square root of the aging time. Since n was taken as 0.5, according to the formula (2), the value of k equal to the square of the slope of the line fitting in Fig. 12. The value of k calculated by the curve slope were 0.355, 0.324 and 0.179 $\mu\text{m}/\text{h}^{1/2}$ (equal to 3.501×10^{-17} , 2.916×10^{-17} and 8.9×10^{-18} m^2/s) for total IMC layer of the SAC305/Cu, SAC305/Cu-30Co and SAC305/Cu-50Co joints, respectively. These results were similar to the relevant research results for Sn3.5Ag0.5Cu/Cu couples, i.e. 7.92×10^{-17} m^2/s with aging treatment at 180 °C [38]. It could be found that the k values for interfacial IMC decreased with the increasing content of Co in substrate.

This means the smaller the value of k , the slower the interfacial IMC grew and the smaller thickness of the reaction layers. Compared with the SAC305/Cu solder joint, it was proved that the Co added to alloying substrate could effectively inhibit the growth of IMCs. It was revealed that the addition of the Co atoms in Cu substrate could effectively reduce the rate of interfacial reaction between solder and substrate, and achieve the purpose of restraining the growth of the interfacial IMCs.

4 Conclusions

In this experiment, the SAC305/Cu- x Co ($x=0, 30$ and 50 wt%) soldered joints were studied during reflowing at 290 °C for 10 min and solid-state treatment at 150 °C for various time. The effects of the addition of Co content in substrate on the growth and the growth kinetics of the interfacial IMC layers were investigated. It was found that the IMC of SAC305/Cu joint consist of Cu_6Sn_5 and Cu_3Sn phase, while the dominating composition of the IMC layers of SAC305/Cu- x Co ($x=30$ and 50 wt%) joint was $(\text{Cu},\text{Co})_6\text{Sn}_5$ and $(\text{Cu},\text{Co})_3\text{Sn}$ phase. Moreover, a little $(\text{Cu},\text{Co})\text{Sn}_2$ phase was found adjacent to the Co-rich phase after soldering and eliminated after the aging treatment.

After the same conditions of solid-state aging treatment, the thicknesses of the IMC layers of the two kinds of joints (SAC305/Cu-30Co and SAC305/Cu-50Co) were much smaller than that of the SAC305/Cu joints. This observation showed that the consuming rate of Cu was faster than that of Co in the Cu-Co substrate, which verified that the alloying of the substrate could inhibit the growth of the total IMC. Moreover, the thickness of the interfacial IMC increased with the increased aging time and was linear with the square root of the aging time. Comparing the SAC305/Cu-30Co and SAC305/Cu-50Co solder joint, the latter shows the smaller thickness of the IMC layers and the lower growth rate. With the content of Co increased in substrate, the more obvious inhibition of the growth of the whole interfacial compounds.

Acknowledgements This work was supported by the Nature Science Foundation of China (nos. 51465039, 51665038, 51765040), Nature Science Foundation of Jiangxi Province (20161BAB206122), Key project of the Nature Science Foundation of Jiangxi Province (20171ACB21011) and Postgraduate Innovation special funds of Jiangxi province (YC2016-S045).

References

1. H.T. Lee, H.S. Lin, C.S. Lee, P.W. Chen, Reliability of Sn-Ag-Sb lead-free solder joints. *Mater. Sci. Eng. A.* **407**, 36–44 (2005)
2. M.N. Islam, Y.C. Chan, M.J. Rizvi, W. Jillek, Investigations of interfacial reactions of Sn-Zn based and Sn-Ag-Cu lead-free

- solder alloys as replacement for Sn–Pb solder. *J. Alloys Compd.* **400**, 136–144 (2005)
3. Y. Fujiwara, H. Enomoto, T. Nagao, H. Hoshika, Composite plating of Sn–Ag alloys for Pb-free soldering. *Surf. Coat. Technol.* **169**, 100–103. (2003)
 4. N.D. Lu, D.H. Yang, L.L. Li, Interfacial reaction between Sn–Ag–Cu solder and Co–P films with various microstructures. *Acta Mater* **61**, 4581–4590 (2013)
 5. C.H. Wang, C.C. Wen, C.Y. Lin, Solid-state interfacial reactions of Sn and Sn–Ag–Cu solders with an electroless Co(P) layer deposited on a Cu substrate. *J. Alloys Compd.* **662**, 475–483 (2016)
 6. T.C. Chang, M.C. Wang, M.H. Hon, Growth and morphology of the intermetallic compounds formed at the Sn–9Zn–2.5Ag/Cu interface. *J. Alloys Compd.* **402**, 141–148 (2005)
 7. F. Gao, T. Takemoto, H. Nishikawa, Effects of Co and Ni addition on reactive diffusion between Sn–3.5Ag solder and Cu during soldering and annealing. *Mater. Sci. Eng. A.* **420**, 39–46 (2006)
 8. M. Yang, Y.H. Ko, J. Bang, T.S. Kim, C.W. Lee, M.Y. Li, Effects of Ag addition on solid–state interfacial reactions between Sn–Ag–Cu solder and Cu substrate. *Mater. Charact.* **124**, 250–259 (2017)
 9. C.H. Wang, K.T. Li, Strong effects of minor Ga addition on liquid state Sn–Ga/Co. *J. Alloys Compd.* **649**, 1197–1204 (2015)
 10. Y.W. Wang, Y.W. Lin, C.T. Tu, C.R. Kao, Effects of minor Fe, Co, and Ni additions on the reaction between SAC305 solder and Cu. *J. Alloys Compd.* **478**, 121–127 (2009)
 11. W.M. Chen, S.K. Kang, C.R. Kao, Effects of Ti addition to Sn–Ag and Sn–Cu solders. *J. Alloys Compd.* **520**, 244–249 (2012)
 12. F. Gao, F.J. Cheng, H. Nishikawa, T. Takemoto, Characterization of Co–Sn intermetallic compounds in Sn–3.0Ag–0.5Cu–0.5Co lead-free solder alloy. *Mater. Lett.* **62**, 2257–2259 (2008)
 13. J.W. Yoon, B.I. Noh, B.K. Kim, C.C. Shur, S.B. Jung, Wettability and interfacial reactions of Sn–Ag–Cu/Cu and Sn–Ag–Ni/Cu solder joints. *J. Alloys Compd.* **486**, 142–147 (2009)
 14. H.K. Cheng, C.W. Huang, H. Lee, Y.L. Wang, T.F. Liu, C.M. Chen, Interfacial reactions between Cu and SAC305 solder doped with minor Ni. *J. Alloys Compd.* **622**, 529–534 (2015)
 15. M.G. Cho, S.K. Seo, H.M. Lee, Wettability and interfacial reactions of Sn-based Pb-free solders with Cu–xZn alloy under bump metallurgies. *J. Alloys Compd.* **474**, 510–516 (2009)
 16. P. Sun, C. Andersson, X.C. Wei, Z.N. Cheng, D. Shangguan, J. Liu, Intermetallic compound formation in Sn–Co–Cu, Sn–Ag–Cu and eutectic Sn–Cu solder joints on electroless Ni(P) immersion Au surface finish after reflow soldering. *Mater. Sci. Eng. B.* **135**, 134–140 (2006)
 17. Y.T. Chen, Y.T. Chan, C.C. Chen, Wettability and interfacial reactions between the molten Sn–3.0 wt%Ag–0.5 wt%Cu solder (SAC305) and Ni–Co alloys. *J. Alloys Compd.* **507**, 419–424 (2010)
 18. W.J. Zhu, J. Wang, H.S. Liu, Z.P. Jin, W.P. Gong, The interfacial reaction between Sn–Ag alloys and Co substrate. *Mater. Sci. Eng. A.* **456**, 109–113 (2007)
 19. C.H. Wang, C.Y. Kuo, Peltier effect on CoSn₃ growth in Sn/Co/Sn couples with different substrate lengths. *Mater. Chem. Phys.* **153**, 72–77 (2015)
 20. N. Zhang, Y.W. Shi, Y.P. Lei, Z.D. Xia, F. Guo, X.Y. Li, Effect of thermal aging on impact absorbed energies of solder joints under high-strain-rate conditions. *J. Electron. Mater.* **38**, 2132–2147 (2009)
 21. X.W. Hu, T. Xu, L.M. Keer, Y.L. Li, X.X. Jiang, Shear strength and fracture behavior of reflowed Sn_{3.0}Ag_{0.5}Cu/Cu solder joints under various strain rates. *J. Alloys Compd.* **690**, 720–729 (2017)
 22. D.Z. Li, C.Q. Liu, P.P. Conway, Characteristics of intermetallics and micromechanical properties during thermal ageing of Sn–Ag–Cu flip-chip solder interconnects. *Mater. Sci. Eng. A.* **391**, 95–103 (2005)
 23. W. Yang, H. Yu, J.H. Wang, C.C. Cai, Z.F. Xu, S. Li, F. Liu, G.C. Yang, Application of dendrite fragmentation to fabricate the homogeneous dispersed structure in undercooled Cu–Co immiscible alloy. *J. Alloys Compd.* **509**, 9675–9678 (2011)
 24. W. Yang, S.H. Chen, H. Yu, S. Li, F. Liu, G.C. Yang, Effects of liquid separation on the microstructure formation and hardness behavior of undercooled Cu–Co alloy. *Appl. Phys. A.* **109**, 665–671 (2012)
 25. W. Yang, Z.F. Xu, W.J. Li, C.C. Cai, S. Li, F. Liu, G.C. Yang, Comparisons of grain refinement and recalescence behavior during the rapid solidification of undercooled Cu–Co and Cu–Ni alloys. *Physica B.* **406**, 3710–3714 (2011)
 26. W. Yang, Y.L. Zhang, W. He, Z.F. Xu, Effects of copper content and liquid separation on the microstructure formation of Co–Cu alloys. *Int. J. Mater. Res.* **105**, 861–868 (2014)
 27. B. Massalski, H. Okamoto, P.R. Subramanian, L. Kacprzak, *Binary Alloy Phase Diagrams*, 2nd edn. (ASM International, Materials Park, OH, 1990)
 28. K.N. Satyanarayan, Prabhu, Effect of temperature and substrate surface texture on wettability and morphology of IMCs between Sn–0.7Cu solder alloy and copper substrate. *J. Mater. Sci. Mater. Electron.* **23**, 1664–1672 (2012)
 29. N. Kiran, K.N. Bhat, Prabhu, Satyanarayan, Effect of reflow temperature and substrate roughness on wettability, IMC growth and shear strength of SAC387/Cu bonds. *J. Mater. Sci. Mater. Electron.* **25**, 864–872 (2014)
 30. Q.Q. Lai, L. Zhang, N. Eustathopoulos, Enhanced wetting of dual-phase metallic solids by liquid metals: a new effect of interfacial reaction. *Acta Mater* **61**, 4127–4134 (2013)
 31. H. Chen, Y.L. Tsai, Y.T. Chang, A.T. Wu, Effect of massive spalling on mechanical strength of solder joints in Pb-free solder reflowed on Co-based surface finishes. *J. Alloys Compd.* **671**, 100–108 (2016)
 32. J.J. Sundelin, S.T. Nurmi, T.K. Lepistö, E.O. Ristolainen, Mechanical and microstructural properties of SnAgCu solder joints. *Mater. Sci. Eng. A.* **420**, 55–62 (2006)
 33. W.G. Yang, R.W. Messler, L.E. Felton, Microstructure evolution of eutectic Sn–Ag solder joints. *J. Electron. Mater.* **23**, 765–772 (1994)
 34. D.Q. Yu, C.M.L. Wu, C.M.T. Law, L. Wang, J.K.L. Lai, Intermetallic compounds growth between Sn–3.5Ag lead-free solder and Cu substrate by dipping method. *J. Alloys Compd.* **392**, 192–199 (2005)
 35. X.W. Hu, Y.L. Li, Z.X. Min, Interfacial reaction and IMC growth between Bi-containing Sn_{0.7}Cu solders and Cu substrate during soldering and aging. *J. Alloys Compd.* **582**, 341–347 (2014)
 36. C.H. Wang, C.Y. Kuo, S.E. Huang, P.Y. Li, Temperature effects on liquid-state Sn/Co interfacial reactions. *Intermetallics* **32**, 57–63 (2013)
 37. C.H. Wang, C.Y. Kuo, Growth kinetics of the solid-state interfacial reactions in the Sn–Cu/Co and Sn/Co–Cu couples. *Mater. Chem. Phys.* **130**, 651–656 (2011)
 38. T. Xu, X.W. Hu, Y.L. Li, X.X. Jiang, The growth behavior of interfacial intermetallic compound between Sn–3.5Ag–0.5Cu solder and Cu substrate under different thermal-aged conditions. *J. Mater. Sci. Mater. Electron.* **25**, 1–14 (2017)